ChemComm

COMMUNICATION

View Article Online
View Journal | View Issue

Cite this: *Chem. Commun.*, 2019, **55**, 11279

Received 11th June 2019,
Accepted 16th August 2019

DOI: 10.1039/c9cc04494a

rsc.li/chemcomm

Turning on ROP activity in a bimetallic Co/Zn complex supported by a [2+2] Schiff-base macrocycle†

Kuiyuan Wang, Timothy J. Prior and Carl Redshaw *

Homo-dinuclear Co and Zn complexes derived from the macrocycle LH_2, {[2-(OH)-5-(R)-C_6H_2-1,3-$(CH)_2$][CH_2CH_2(2-$C_6H4N)_2$]}$_2$ (R = Me, *t*Bu), revealed near inactivity for the ring opening polymerization (ROP) of the cyclic esters δ-valerolactone (δ-VL) and ε-caprolactone (ε-CL). By contrast, the hetero-bimetallic complexes [LCo(NCMe)(μ-Br)ZnBr]·*n*MeCN (*n* = 3 or 3.25) were found to be efficient catalysts for the ROP of ε-CL and δ-VL.

The production of aliphatic polyesters has become a very topical area given their biodegradability and biocompatibility,[1] and given the current global issues with plastic pollution, this is likely to remain the case for the foreseeable future.[2] One viable route to such polymers is *via* the metal-catalyzed ring opening polymerization (ROP) of cyclic esters.[3] The choice of metal catalyst is influenced by a number factors, such as price, toxicity, activity and control. Frameworks that are capable of simultaneously binding multiple metal centres continue to be of great interest in various fields of catalysis, and this stems from the possible presence of favourable cooperative effects.[4] We have become interested in the use of Schiff-base macrocycles given that they possess multiple binding sites,[5] and our studies have been focusing on the simplest members of this family, the so-called Robson type macrocycles, derived from the [2+2] condensation of a diamine/dianiline with a dialdehyde.[6] In terms of catalysis (ROP of ε-CL), we observed beneficial cooperative effects when alkylaluminium centres are bound in a specific way to a Schiff-base macrocycle (LH_2, Scheme 1, left) derived from the dianiline [$(CH_2CH_2)(2\text{-}C_6H_4NH_2)_2$], whereas the presence of aluminoxane type (Al–O–Al) bonding in such a system proved detrimental.[7] Furthermore, we noted that manganese complexes of such macrocycles were far less active with conversions for the ROP of ε-CL <15%.[8] It is noteworthy that the structural chemistry of this particular macrocycle is underexplored, indeed a search of the CSD revealed no hits,[9] other than our previously mentioned chemistry.[7,8] We have selected the metals cobalt and zinc given their relatively low cost and biocompatibility. Further, we note that the use of Zn complexes for the ROP of ε-CL is well established,[3] whilst reports on ROP using Co species is scant.[10]

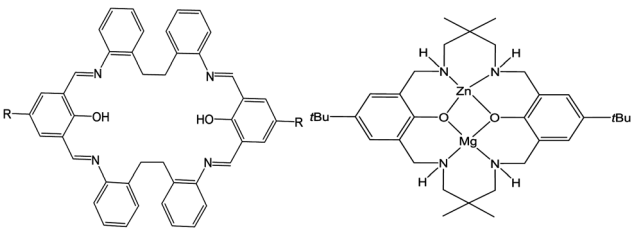

Scheme 1 Macrocycle LH_2 (R = Me, *t*Bu) and the Zn–Mg complex reported by Williams *et al.*

Recent work by Williams *et al.* has shown how the use of hetero-dinuclear complexes can result in enhanced catalytic performance.[11a] In particular, it was reported that an *in situ* generated catalyst comprising the hetero-dinuclear Zn–Mg complex bearing a diphenolate tetraamine macrocycle (Scheme 1, right) used in conjunction with its homo-dinuclear Zn–Zn and Mg–Mg counterparts performed better for the copolymerization of CO_2 with epoxides than did the homo-dinuclear complexes alone. Given the very similar solubility properties of the three species, it was not possible to crystallize selectively the Mg–Zn hetero-dinuclear complex. However, subsequent studies by the same group have shown that it is possible to access such species *via* mono-metalation, followed by the addition of the second metal,[11b] and the molecular structures of a number of mixed-metal species were reported.[11c–e] Interestingly, Williams *et al.* also observed that for ROP of ε-CL and *r*-LA, a mixed Ti/Zn system displayed moderate/high activity whilst the mono-Ti system was inactive.[11c] We also note that cooperative effects have also been observed for a homo-dinuclear zinc complex in lactide polymerization.[12]

Given this, we have re-focused our efforts on the [2+2] Schiff-base systems and have extended our studies in an attempt to

Department of Chemistry & Biochemistry, University of Hull, Hull, HU6 7RX, UK. E-mail: c.redshaw@hull.ac.uk; Tel: +44 1482 465219

† Electronic supplementary information (ESI) available: Full experimental details for complex synthesis and ROP studies. CCDC 1829365–1829367 (**1*t*Bu**·0.5MeCN, **2*t*Bu**·4.5MeCN, and **5*t*Bu**·3.25MeCN), 1849421 (**4*t*Bu**·0.25MeCN) and 1921189–1921192. For ESI and crystallographic data in CIF or other electronic format see DOI: 10.1039/c9cc04494a

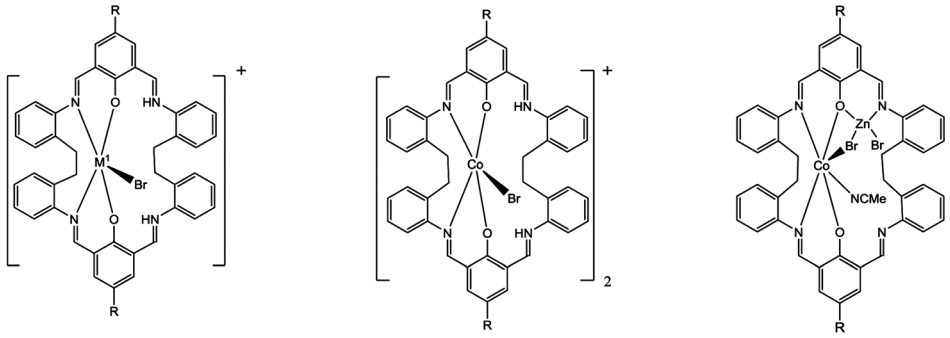

Scheme 2 Cobalt and zinc complexes **1–5** prepared herein.

access mixed-metal systems. Herein, we report that homo-dinuclear cobalt and zinc complexes bearing the macrocycle L (**1–3**, Scheme 2) are readily accessible. Furthermore, on reacting **1** with Br_2Zn a complex **4** related to **1** was formed differing only in the composition (partial occupancy Co : Zn = 68 : 32) of the anion, whereas with Et_2Zn, it proved possible to isolate and structurally characterize the mixed-metal Co–Zn complexes **5** (Scheme 2 right). Interestingly, the homo-dinuclear species **1** and **3** (R = Me and *t*Bu) were inactive when screened for the ROP of ε-CL (and virtually inactive for ε-VL), whereas the mixed-metal complexes **5Me** and **5*t*Bu** were efficient catalysts when screened under the same conditions (130 °C, 24 h). We note that poly(ε-caprolactone), PCL and PVL are favoured polymers given both their biodegradability, and are considered as potential environmentally friendly commodity plastics.[13] Beyond ROP, Co–Zn species are of interest in gas sensors, semiconductors, dyes and pigments, as well as in other catalytic processes.[14]

Reaction of the [2+2] Schiff-base macrocycle {[2-(OH)-5-(R)-C_6H_2-1,3-$(CH)_2$][CH_2CH_2(2-C_6H_4N)$_2$]}$_2$ (R = Me, *t*Bu) with 2.1 equivalents of $CoBr_2$ afforded, following work-up, green prisms on recrystallization from a saturated solution of acetonitrile at 0 °C in about 70% yield. The molecular structure of **1*t*Bu**·0.5MeCN is shown in Fig. 1, with selected bond lengths and angles given in the caption; for **1Me**·4MeCN see ESI,† Fig. S1. The complex is a salt of formula [CoBr**L**$^{t\mathbf{Bu}}$][$CoBr_3$(NCMe)]·0.5MeCN (**1*t*Bu**·0.5MeCN). In the cation, the cobalt centre is five-coordinate with a trigonal bipyramidal geometry; the apical sites are occupied by O atoms of phenolates, with the bromide and two N atoms in the equatorial sites. Concentration of the mother-liquor afforded more of **1*t*Bu**·0.5MeCN plus small amounts of an orange/red product, identified as [CoBr**L**$^{t\mathbf{Bu}}$]$_2$[$CoBr_3$(NCMe)][Br]·4.5MeCN (**2*t*Bu**·4.5MeCN), the structure of which is similar to that observed for **1*t*Bu**·0.5MeCN, differing mainly in the composition of the anions, namely Br^- and $CoBr_3(NCMe)^-$; the molecular structure is shown in Fig. S2 (ESI†). Similar interaction of LH_2 with 2.1 equivalents of $ZnBr_2$ afforded, following work-up, yellow prisms of [Zn**L**$^{t\mathbf{Bu}}$Br][$ZnBr_3$(NCMe)]·MeCN (**3*t*Bu**·MeCN) in good yield. Use of excess $ZnBr_2$ (>4 equivalents) also afforded **3*t*Bu**·MeCN as the only crystalline product. Again, the structure (ESI,† Fig. S4) is very reminiscent of **1*t*Bu**·0.5MeCN, with the zinc adopting a trigonal bipyramidal geometry in the cation; for the structure of **3Me**·MeCN, see Fig. S3 (ESI†). Having isolated and characterized these homo-dinuclear products, we then targeted the formation of a mixed-metal system. Complex **1*t*Bu** was reacted with $ZnBr_2$ to afford a yellow product, however the structure, namely [CoBr**L**$^{t\mathbf{Bu}}$][$Co_{0.68}Zn_{0.32}Br_3$(NCMe)]·0.25MeCN (**4*t*Bu**·0.25MeCN), turned out to be very similar to **1** differing only in the composition of the anion, the latter having cobalt : zinc occupancy 68.4 : 32.6(17) (ESI,† Fig. S5). We note that the structures of both **3Me**/**3*t*Bu** and **4*t*Bu** are analogous to the equivalent manganese complex (see CUVYID in CCDC).[7c] Given this disappointing result, both **1Me** and **1*t*Bu** were treated with Et_2Zn (one equivalent) and on work-up (acetonitrile), brown/red products were isolated in good yield. Single crystals were grown from acetonitrile on prolonged standing (3 days) at ambient temperature. The molecular structure of **5*t*Bu**·3.25MeCN is shown in Fig. 2, with bond lengths/angles given in the caption; for **5Me**·3MeCN see Fig. S6, ESI.† In **5*t*Bu**·3.25MeCN, the macrocycle binds two metals (Co and Zn) in an ordered way. The Co^{2+} is bound in distorted octahedral geometry by two *cis* phenolates and two *cis* imines of the macrocycle, a rather distant bromide (Co(1)–Br(1) 2.9383(5) Å), and a single

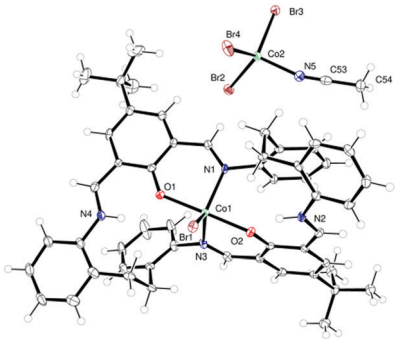

Fig. 1 Molecular structure of **1*t*Bu**·0.5MeCN. Solvent omitted for clarity. Thermal ellipsoids are drawn at the 30% probability level. Selected bond lengths (Å) and angles (°): Co(1)–Br(1) 2.4847(6), Co(1)–O(1) 2.004(2), Co(1)–O(2) 2.043(2), Co(1)–N(1) 2.088(3), Co(1)–N(3) 2.105(3); O(1)–Co(1)–O(2) 178.52(9), N(1)–Co(1)–N(3) 108.77(11), O(1)–Co(1)–Br(1) 92.98(7), N(3)–Co(1)–Br(1) 128.17(8), N(1)–Co(1)–Br(1) 122.54(8), N(1)–Co(1)–N(3) 108.77(11).

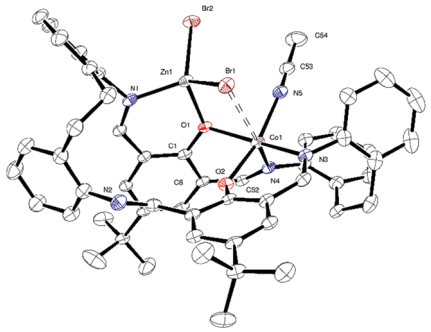

Fig. 2 The molecular structure of **5*t*Bu**·3.25MeCN. Solvent omitted for clarity. Thermal ellipsoids are drawn at the 30% probability level. Selected bond lengths (Å) and angles (°): Co(1)–O(1) 2.133(2), Co(1)–O(2) 1.947(2), Co(1)–N(3) 2.058(2), Co(1)–N(4) 2.126(2), Co(1)–N(5) 2.108(3), Zn(1)–Br(1) 2.3873(4), Zn(1)–Br(2) 2.3412(5), Zn(1)–O(1) 1.9792(19), Zn(1)–N(1) 2.015(3); Co(1)–O(1)–Zn(1) 103.93(8), N(3)–Co(1)–N(4) 107.92(9), O(2)–Co(1)–N(3)90.50(9), O(2)–Co(1)–N(5) 167.52(9), O(1)–Zn(1)–N(1) 93.30(9), Br(1)–Zn(1)–Br(2) 113.655(18).

molecule of acetonitrile. The Zn ion is in close proximity to the Co ion: the bromide and one of the phenolates each coordinate to the Zn. The tetrahedral coordination about the Zn is completed by an imine and a mono-dentate bromide. One might describe the octahedron of Co(1) and the tetrahedron around Zn(1) as sharing a common edge (O(1) and Br(1)). The two metals are separated at a distance 3.2399(5) Å. The magnetic moments of **5** (R = Me, *t*Bu) are in the range 5.1–5.3 μ_B

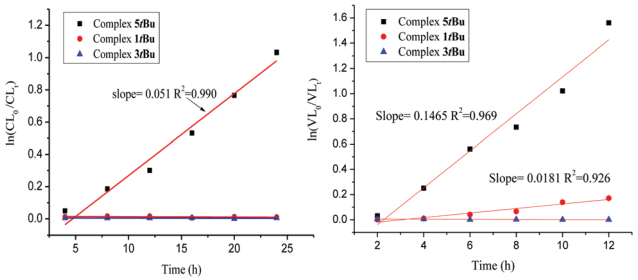

Fig. 3 Plot of $\ln[VL]_0/[VL]_t$ *vs.* time and $\ln[CL]_0/[CL]_t$ *vs.* time using complex **1*t*Bu**, **3*t*Bu** and **5*t*Bu** ([monomer] : [Cat] : [BnOH] = 500 : 1 : 1); 130 °C.

consistent with high spin Co(II) complexes,[15] whilst the ^{1}H NMR spectra are broad and spread over a large window (+140 to −40 ppm). The cobalt and zinc complexes **1**, **3** and **5** (R = Me, *t*Bu) have been screened for their ability to ring open polymerize δ-VL and ε-CL; runs were conducted in the presence of benzyl alcohol (BnOH). For complexes **1** and **3**, a variety of conditions were used in the attempted ROP of δ-VL including temperatures in the range 40 to 130 °C, differing ratios of [δ-VL] : [Cat] : [BnOH] and over different times, however on each occasion there was no sign of polymer upon work-up. However, for the mixed-metal system **5**, activity was observed when the temperature reached 130 °C, in the presence of one equivalent of BnOH (at this temperature, no activity was observed for **1** and **3** – see Fig. 3 for the relative rates of the *t*Bu derivatives). Data for runs is given in Table 1 (see also Fig. S19–S24, ESI†) and reveals that **5*t*Bu** out-performs **5Me**, which is thought to be due to the increased solubility of the former in the reaction solvent. In these mixed-metal systems, the Co to Zn distance may favour coordination of a monomer to both metal centres, and then as in the ROP of propylene oxide,[16] one metal acts a as Lewis acid with the other using its M-OR function to attack the carbonyl group. Highest conversions were achieved with ratios between 100 : 1 : 1 and 500 : 1 : 1 at 130 °C, with all the runs showing good control with PDIs in range 1.15–1.30; above and below this temperature only trace polymer was observed. Use of either 12 h (run 6) or no solvent (*i.e.* a melt, run 7) was less controlled. Analysis of the polymer indicated the presence of benzyloxy and hydroxyl end groups (Fig. S22, ESI†). There was evidence of transesterification and all observed M_n values were significantly lower than the calculated values (see Fig. S21, ESI†). In the case of ε-CL, the situation was more pronounced with no conversion evident by ^{1}H NMR spectroscopy for catalyst systems **1** and **3**. By contrast, systems using **5Me** and **5*t*Bu** were efficient catalysts at 130 °C over 24 h, with similar conversion results observed using the ratios between 50 : 1 : 1 and 500 : 1 : 1; above and below this temperature only trace polymer was observed. As for the δ-VL runs, good control was observed, except for when using either 12 h or a melt. From a kinetic study, it was observed that the polymerization rate exhibited near first order dependence of the CL concentration at 130 °C. The rate of polymerization for ε-CL (K_{obs} = 2.12 × 10^{-3} (h^{-1}) for **5*t*Bu**) was less than half that for δ-VL (K_{obs} = 6.10 × 10^{-3} (h^{-1}) for **5*t*Bu**),

Table 1 ROP of δ-VL using complexes **1–5**

Run	Cat.	[δ-VL] : [Cat] : [BnOH]	*T* (°C)	*t* (h)	Conv.[a] (%)	$M_n \times 10^{3}$ [b]	$M_{nCalcd} \times 10^{4}$ [c]	PDI[d]
1	**5*t*Bu**	50 : 1 : 1	130	24	88.7	1.35	0.45	1.16
2	**5*t*Bu**	100 : 1 : 1	130	24	92.8	2.14	0.93	1.15
3	**5*t*Bu**	250 : 1 : 1	130	24	98.7	5.19	2.46	1.22
4	**5*t*Bu**	500 : 1 : 1	130	24	99.4	6.89	4.97	1.23
5	**5*t*Bu**	1000 : 1 : 1	130	24	77.9	5.33	7.79	1.43
6	**5*t*Bu**	500 : 1 : 1	130	12	92.7	0.45	4.64	1.53
7	**5*t*Bu**	500 : 1 : 1 (melt)	130	24	96.2	7.11	4.82	1.79
8	**5*t*Bu**	500 : 1 : 1	70	24	76.1	0.76	3.80	1.19
9	**5Me**	250 : 1 : 1	130	24	97.0	2.68	2.43	1.30
10	**5Me**	500 : 1 : 1	130	24	91.4	3.35	4.57	1.15
11	**1*t*Bu**	500 : 1 : 1	130	24	38.8	0.45	1.94	1.42
12	**3*t*Bu**	500 : 1 : 1	130	24	4.4	—	0.22	—

[a] By ^{1}H NMR spectroscopic analysis. [b] M_n values were determined by GPC in THF *vs.* PS standards and were corrected with a Mark–Houwink factors (0.58 for poly(δ-VL)). [c] (F.W.[M]/[BnOH])(conversion). [d] Polydispersity index (M_w/M_n) were determined by GPC.

Table 2 ROP of ε-CL using complexes **1–5**

Run	Cat.	[ε-CL] : [Cat] : BnOH	T (°C)	t (h)	Conv.[a] (%)	$M_n \times 10^{3}$ [b]	$M_{nCalcd} \times 10^{4}$ [c]	PDI[d]
1	**5*t*Bu**	50 : 1 : 1	130	24	99.3	1.14	0.57	1.14
2	**5*t*Bu**	100 : 1 : 1	130	24	99.6	2.65	1.01	1.13
3	**5*t*Bu**	250 : 1 : 1	130	24	99.6	4.10	2.86	1.13
4	**5*t*Bu**	500 : 1 : 1	130	24	99.8	6.56	5.05	1.34
5	**5*t*Bu**	1000 : 1 : 1	130	24	88.7	3.61	8.87	1.12
6	**5*t*Bu**	500 : 1 : 1	130	12	48.0	2.28	2.74	1.80
7	**5*t*Bu**	500 : 1 : 2	130	24	71.5	3.48	1.78	1.15
8	**5*t*Bu**	500 : 1 : 1 (melt)	130	24	98.2	7.87	4.98	1.66
9	**5*t*Bu**	500 : 1 : 1	70	24	72.7	—	3.63	—
10	**5Me**	250 : 1 : 1	130	36	97.6	4.83	2.44	1.34
11	**5Me**	500 : 1 : 1	130	36	99.2	5.16	4.96	1.96
12	**1*t*Bu**	500 : 1 : 1	130	24	—	—	—	—
13	**1Me**	500 : 1 : 1	130	24	—	—	—	—

[a] By ^{1}H NMR spectroscopic analysis. [b] M_n values were determined by GPC in THF *vs.* PS standards and were corrected with a Mark–Houwink factors (0.56 for poly(ε-CL)). [c] (F.W.[M]/[BnOH])(conversion). [d] Polydispersity index (M_w/M_n) were determined by GPC.

which is consistent with other reports.[17] The observed molecular weights were lower than the calculated values, suggesting the presence of a chain transfer agent (H_2O or BnOH). This was also evident in the MALDI-TOF mass spectra, were a number of families of peaks were observed separated by 114 mass units (Fig. S26 and S27, ESI†); the highest were typically about 7000. For example, in the case of **5*t*Bu** (run 4, Table 2), peaks in the spectrum can be assigned to 4926, 5039, and 5154 using the formula C_6H_6–$CH_2O[O(CH_2)_4CO]_nOH$ for n = 42, 43 and 44 respectively. The ^{1}H NMR spectra of the PCL (*e.g.* Fig. S28, ESI†) revealed the presence of benzyloxy and OH end groups. It also proved possible to ROP *r*-LA using the mixed-metal systems, albeit in much poorer yields. Moreover, co-polymerization of ε-VL and ε-CL was possible as was ε-CL with *r*-LA (see Table S1 and Fig. S33–S43, ESI† for preliminary results).

In conclusion, we have isolated and structurally characterized homo-dinuclear cobalt and zinc complexes as well as rare examples of mixed-metal (Co/Zn) complexes of a [2+2] macrocyclic Schiff-base. Screening of these complexes for the ROP of the cyclic esters δ-valerolactone (δ-VL) and ε-caprolactone (ε-CL) revealed that whilst the homo-dinuclear complexes are either virtually inactive (δ-VL) or inactive (ε-CL), the mixed-metal systems are efficient catalysts at 130 °C, suggestive that the metals are able to 'turn each other on'.

We thank the China Scholarship Council (CSC) for a PhD Scholarship with KW. CR thanks the EPSRC (grant EP/S025537/1) for financial support. We thank the EPSRC National Crystallography Service for data collection and the Physical Sciences Data-Science Service for access to the CCDC.

Conflicts of interest

There are no conflicts to declare.

References

1 A. C. Albertsson and I. K. Varma, *Biomacromolecules*, 2003, **4**, 1466–1486.
2 P. Villarrubia-Gómez, S. E. Cornell and J. Fabres, *Marine Policy*, 2018, **96**, 213–220.
3 For reviews, see (*a*) O. Dechy-Cabaret, B. Martin-Vaca and D. Bourissou, *Chem. Rev.*, 2004, **104**, 6147–6176; (*b*) M. Labet and W. Thielemans, *Chem. Soc. Rev.*, 2009, **38**, 3484–3504; (*c*) C. M. Thomas, *Chem. Soc. Rev.*, 2010, **39**, 165–173; (*d*) A. Arbaoui and C. Redshaw, *Polym. Chem.*, 2010, **1**, 801–826; (*e*) Y. Sarazin and J.-F. Carpentier, *Chem. Rev.*, 2015, **115**, 3564–3614 and references therein.
4 See for example, (*a*) S. K. Mandal and H. W. Roesky, *Acc. Chem. Res.*, 2010, **43**, 248–259; (*b*) M. Delferro and T. J. Marks, *Chem. Rev.*, 2011, **111**, 2450–2485; (*c*) J. P. McInnis, M. Delferro and T. J. Marks, *Acc. Chem. Res.*, 2014, **47**, 2545–2557; (*d*) I. Bratko and M. GÓmez, *Dalton Trans.*, 2013, **42**, 10664–10681.
5 (*a*) S. Brooker, *Coord. Chem. Rev.*, 2001, **222**, 33–56; (*b*) W. Radecka-Paryzek, V. Patroniak and J. Lisowski, *Coord. Chem. Rev.*, 2005, **249**, 2156–2175; (*c*) C. Redshaw, *Dalton Trans.*, 2016, **45**, 9018–9030; (*d*) C. Redshaw, *Catalysts*, 2017, **7**, 165.
6 (*a*) N. H. Pilkington and R. Robson, *Aust. J. Chem.*, 1970, **23**, 2225–2236; (*b*) M. Bell, A. J. Edwards, B. F. Hoskins, E. H. Kachab and R. Robson, *J. Am. Chem. Soc.*, 1989, **111**, 3603–3610.
7 (*a*) A. Arbaoui, C. Redshaw and D. L. Hughes, *Chem. Commun.*, 2008, 4717; (*b*) A. Arbaoui, C. Redshaw and D. L. Hughes, *Supramol. Chem.*, 2009, **21**, 35; (*c*) W. Yang, K.-Q. Zhao, B.-Q. Wang, C. Redshaw, M. R. J. Elsegood, J.-L. Zhao and T. Yamato, *Dalton Trans.*, 2016, **45**, 11990–12005.
8 W. Yang, K.-Q. Zhao, B.-Q. Wang, C. Redshaw, M. R. J. Elsegood, J.-L. Zhao and T. Yamato, *Dalton Trans.*, 2016, **45**, 226–236.
9 F. H. Allen, *Acta Crystallogr., Sect. B: Struct. Sci.*, 2002, **58**, 380.
10 See for example, J. Zhang, B. Wang, L. Wang, J. Sun, Y. Zhang, Z. Cao and Z. Wu, *Appl. Organomet. Chem.*, 2018, 32e4077 and references therein.
11 (*a*) P. K. Saini, C. Romain and C. K. Williams, *Chem. Commun.*, 2014, **50**, 4164–4167; (*b*) J. F. Garden, P. K. Saini and C. K. Williams, *J. Am. Chem. Soc.*, 2015, **137**, 15078–15081; (*c*) J. F. Garden, A. J. P. White and C. K. Williams, *Dalton Trans.*, 2017, **46**, 2532–2541; (*d*) A. C. Deacy, C. B. Durr, J. F. Garden, A. J. P. White and C. K. Williams, *Inorg. Chem.*, 2018, **57**, 15575–15583; (*e*) G. Trott, J. F. Garden and C. K. Williams, *Chem. Sci.*, 2019, **10**, 4618–4627.
12 A. Thevenon, C. Romain, M. S. Bennington, A. J. P. White, H. J. Davidson, S. Brooker and C. K. Williams, *Angew. Chem., Int. Ed.*, 2016, **55**, 8680–8685.
13 See for example, (*a*) M. A. Woodruff and D. W. Hutmacher, *Prog. Polym. Sci.*, 2010, **35**, 1217–1256; (*b*) Y. F. Al-Khafaji and F. H. Hussein in *Green and Sustainable Advanced Materials: Processing and Characterization*, ed. S. Ahmed and C. M. Hussain, Wiley, 2018, ch. 6.
14 (*a*) T. Baird, K. C. Campbell, P. J. Holliman, R. W. Hoyle, D. Stirling, B. P. Williams and M. Morris, *J. Mater. Chem.*, 1997, **7**, 319–330; (*b*) X. Niu, W. Du and W. Du, *Sens. Actuators, B*, 2004, **99**, 405–409; (*c*) N. H. Perry, T. O. Mason, C. Ma, A. Navrotsky, S. A. Kondrat, T. E. Davies, D. J. Morgan, D. I. Enache, G. B. Combes, S. H. Taylor, J. K. Bartley and G. J. Hutchings, *Catal. Sci. Technol.*, 2014, **4**, 1970–1978.
15 (*a*) R. W. Handel, H. Willms, G. B. Jameson, K. J. Berry, B. Moubaraki, K. S. Murray and S. Brooker, *Eur. J. Inorg. Chem.*, 2010, 3317–3327; (*b*) A. A. Abou-Hussein and W. Linert, *Spectrochim. Acta, Part A*, 2015, **141**, 223–232.
16 (*a*) B. Antelmann, M. H. Chisholm, S. S. Iyer, J. C. Huffman, D. Navarro-Llobet, M. Pagel, W. J. Simonsick and W. Zhong, *Macromolecules*, 2001, **34**, 3159–3175; (*b*) W. Braune and J. Okuda, *Angew. Chem., Int. Ed.*, 2003, **42**, 64–68.
17 K. Makiguchi, T. Satoh and T. Kakuchi, *Macromolecules*, 2011, **44**, 1999–2005.